AD-A187 262 CORROSION BEHAVIOR OF SPUTTER-DEPOSITED ALUMINUM-BASED 1/1
ALLOYS EXPOSED TO..(U) MARTIN MARIETTA LABS BALTIMORE
MD W C MOSHIER ET AL. 30 SEP 87 MML-TR-87-75C
UNCLASSIFIED N00014-85-C-0638 F/G 11/6.1 NL

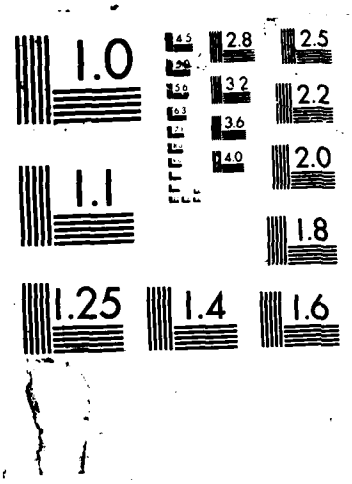
1.0
1.1
1.25
1.4
1.6
1.8
2.0
2.2
2.5
2.8
3.2
3.6
4.0

MML TR [illegible]

CORROSION BEHAVIOR OF SPUTTER-DEPOSITED ALUMINUM ALLOYS EXPOSED TO CHLORIDE SOLUTIONS

Annual Report

[illegible]

[illegible]

Prepared for:

Office of Naval Research
800 North Quincy Street
Arlington, Virginia [illegible]

[illegible]

[illegible]

[illegible]

Martin Marietta [illegible]
Martin Marietta [illegible]
[illegible]
[illegible]

[illegible]

Unclassified
SECURITY CLASSIFICATION OF THIS PAGE

REPORT DOCUMENTATION PAGE

1a. REPORT SECURITY CLASSIFICATION Unclassified	1b. RESTRICTIVE MARKINGS None
2a. SECURITY CLASSIFICATION AUTHORITY	3. DISTRIBUTION / AVAILABILITY OF REPORT Unlimited
2b. DECLASSIFICATION / DOWNGRADING SCHEDULE None	
4. PERFORMING ORGANIZATION REPORT NUMBER(S) MML TR 87-75c	5. MONITORING ORGANIZATION REPORT NUMBER(S)
6a. NAME OF PERFORMING ORGANIZATION Martin Marietta Corporation Martin Marietta Laboratories 6b. OFFICE SYMBOL (*If applicable*) MML	7a. NAME OF MONITORING ORGANIZATION Defense Contract Administration Services Management Area-Baltimore
6c. ADDRESS (*City, State, and ZIP Code*) 1450 South Rolling Road Baltimore, Maryland 21227-3898	7b. ADDRESS (*City, State, and ZIP Code*) 300 East Joppa Road Baltimore, Maryland 21204-3099
8a. NAME OF FUNDING / SPONSORING ORGANIZATION Office of Naval Research 8b. OFFICE SYMBOL (*If applicable*) ONR	9. PROCUREMENT INSTRUMENT IDENTIFICATION NUMBER N00014-85-C-0638
8c. ADDRESS (*City, State, and ZIP Code*) 800 North Quincy Street Arlington, VA 22217-5000	10. SOURCE OF FUNDING NUMBERS PROGRAM ELEMENT NO. / PROJECT NO. / TASK NO / WORK UNIT ACCESSION NO
11. TITLE (*Include Security Classification*) Corrosion Behavior of Sputter-Deposited Aluminum-Based Alloys Exposed to Chloride Solutions	
12. PERSONAL AUTHOR(S) W.C. Moshier, G.D. Davis, G.O. Cote, H.F. Hough and M.E. Vogelsang	
13a. TYPE OF REPORT Annual 13b. TIME COVERED FROM 7/1/86 TO 6/30/87	14. DATE OF REPORT (*Year, Month, Day*) 1987, September, 30 15. PAGE COUNT
16. SUPPLEMENTARY NOTATION	
17. COSATI CODES FIELD / GROUP / SUB-GROUP	18. SUBJECT TERMS (*Continue on reverse if necessary and identify by block number*) Approved for public release; distribution unlimited. Reproduction in whole or in part is permitted for any purpose of the United States Government

19. ABSTRACT (*Continue on reverse if necessary and identify by block number*)

In the second year of the program, the investigation of the passivity of sputter-deposited Al alloys has been extended from Al-Mo and Al-Cr to include Al-Ta, Al-Zr, Al-Si, and Al-Cu. Al-Ta was found to have the greatest effect on the breakdown potential of Al. Al-Mo, Al-Zr, and Al-Cr also substantially impact the breakdown potential, whereas Al-Cu and Al-Si have little or no effect.

A more extensive study of the corrosion behavior of Al-Mo and Al-Cr was performed in salt spray and pit initiation tests. Whereas the Al-Cr alloys outperformed the Al-Mo alloys in the salt spray tests, both alloys were substantially more resistant to attack than pure aluminum. Pit initiation tests showed that the order of the reaction between the alloys and pure Al was identical. However, the time required to initiate a pit was substantially longer for Al-Mo than for Al-Cr or pure Al, indicating that the mechanism by which pits nucleate and grow through the film may be different.

(over)

20. DISTRIBUTION / AVAILABILITY OF ABSTRACT ☒ UNCLASSIFIED/UNLIMITED ☐ SAME AS RPT ☐ DTIC USERS	21. ABSTRACT SECURITY CLASSIFICATION Unclassified
22a. NAME OF RESPONSIBLE INDIVIDUAL Dr. William C. Moshier	22b. TELEPHONE (*Include Area Code*) (301) 247-0700 ext. 2456 22c. OFFICE SYMBOL

☆ U.S. Government Printing Office: 1986—607-044

The changes in the chemistry of the passive film that forms on Al, Al-Mo, and Al-Cr alloys, as a function of solute concentration and applied potential in 0.1 N KCl, were studied. The results show that the mechanisms by which the solute protects the Al alloy differ. Molybdenum forms a film containing MoO_4^{-2}, which impedes the ingress and subsequent movement of the Cl^- anion. In contrast, Cr forms a $Cr(OH)_3$ barrier layer that inhibits the oxidation of the Al substrate and restricts the Cl^- anion from reaching the metal/film interface. Pitting of Al-Mo alloys occurs when sufficient MoO_4^{-2} is replaced by hydrated Mo compounds, whereas pitting of the Al-Cr alloys occurs when Cr^{+3} is oxidized to the more subtle Cr^{+6} state.

MML TR 87-75c

CORROSION BEHAVIOR OF SPUTTER-DEPOSITED ALUMINUM-BASED ALLOYS EXPOSED TO CHLORIDE SOLUTIONS

Annual Report

Period:
July 1, 1986 - June 30, 1987

Prepared for:

Office of Naval Research
800 North Quincy Street
Arlington, Virginia 22217-5000

Under Contract No. N00014-85-C-0638

Submitted by:

W.C. Moshier, G.D. Davis, G.O. Cote, H.F. Hough, and M.E. Vogelsang

MARTIN MARIETTA CORPORATION
Martin Marietta Laboratories
1450 South Rolling Road
Baltimore, Maryland 21227

September 1987

TABLE OF CONTENTS

LIST OF TABLES

LIST OF FIGURES

ABSTRACT

In the second year of the program, the investigation of the passivity of sputter-deposited Al alloys has been extended from Al-Mo and Al-Cr to include Al-Ta, Al-Zr, Al-Si, and Al-Cu. Al-Ta was found to have the greatest effect on the breakdown potential of Al. Al-Mo, Al-Zr, and Al-Cr also substantially impact the breakdown potential, whereas Al-Cu and Al-Si have little or no effect.

A more extensive study of the corrosion behavior of Al-Mo and Al-Cr was performed in salt spray and pit initiation tests. Whereas the Al-Cr alloys outperformed the Al-Mo alloys in the salt spray tests, both alloys were substantially more resistant to attack than pure aluminum. Pit initiation tests showed that the order of the reaction between the alloys and pure Al was identical, indicating that the onset of the pitting process was similar in each case. However, the time required to initiate a pit was substantially longer for Al-Mo than for Al-Cr or pure Al, indicating that the mechanism by which pits nucleate and grow through the film may be different.

The changes in the chemistry of the passive film that forms on Al, Al-Mo, and Al-Cr alloys, as a function of solute concentration and applied potential in 0.1 N KCl, were studied. The results show that the mechanisms by which the solute protects the Al alloy differ. Molybdenum forms a film containing MoO_4^{-2}, which impedes the ingress and subsequent movement of the Cl^- anion. In contrast, Cr forms a $Cr(OH)_3$ barrier layer that inhibits the oxidation of the Al substrate and restricts the Cl^- anion from reaching the metal/film interface. Pitting of Al-Mo alloys occurs when sufficient MoO_4^{-2} is replaced by hydrated Mo compounds, whereas pitting of the Al-Cr alloys occurs when Cr^{+3} is oxidized to the more soluble Cr^{+6} state.

I. INTRODUCTION

Aluminum and its alloys are known for their poor resistance to localized attack and, in particular, for pitting in aqueous chloride-containing environments. Pit formation is caused by the breakdown of the passive film in the presence of chlorides due to its interaction and chemical reaction with the chloride anion. This results in the formation of a more soluble, and therefore less protective film, which eventually leads to the rapid localized dissolution of Al metal and the formation of a pit.

Elements like Mo or Cr promote passivity in Al if they can be retained in solid solution without forming precipitates, which can serve as active microgalvanic cells. These additions can be retained in solid solution by several non-equilibrium alloying techniques (1-4). Since the corrosion behavior of Al is dependent upon the protective properties of the passive film, the presence of these elements improves the protective nature of the film by decreasing its susceptibility to pitting attack.

In the second year of the program, a number of different elements, such as Ta, Zr, Cr, Mo, Cu and Si, were added to Al in various concentrations to study their impact on the alloys' corrosion behavior. Not all of the elements improved the pitting behavior of the alloy. Ta, Zr, Cr, or Mo addition resulted in more noble breakdown (E_b), or pitting, potentials, whereas Si and Cu had little impact on E_b. A detailed study of pit initiation was also performed on Al, Al-1.5Cr, and Al-1.5Mo alloys in solutions containing various concentrations of chlorides.

Changes in the passive film were studied by monitoring the products of the reactions on Al and several Al-Mo and Al-Cr alloys using X-ray photoelectron spectroscopy (XPS), a surface-sensitive technique that has been widely used to study the chemistry of passive films (4-12). This technique provided a quantitative analysis of the passive film and yielded information regarding the oxidation state of the elemental species present, thereby pro-

viding insight into the nature of the chemical changes that occurred during passivation and film breakdown in the presence of chlorides. The changes in the surface chemistry were used to study the mechanism by which these alloying additions affect the passive behavior of Al in aqueous chloride environments.

II. EXPERIMENTAL PROCEDURE

Thin alloy films were prepared by using a RF-magnetron sputter-deposition process. Details regarding the preparation of the alloy films were presented previously (4). Films containing Al and either Mo, Cr, Ta, Zr, Cu, or Si were deposited onto a 2-in.-diam. polished Si single-crystal substrate. The purity of the targets was 99.999% and the concentrations of both oxygen and carbon in the films were below the XPS detectability limits during sputter-depth profiling (less than 1 at.% of the bulk alloy). The alloying additions were co-deposited onto the wafer with the Al to a thickness of 1 μm. The power was 360 W on the Al target and 40 W on the alloying addition target. The range of solute concentration across each wafer at the 360 W/40 W ratio is shown in Table 1. Additional power settings were used on the Mo and Cr targets to form alloys with a wider range of solute concentration. Three different concentrations of Mo- or Cr-containing Al alloys, as well as pure Al, were studied during this program. The solute concentrations (determined by atomic absorption) ranged from 2 to 16 at.% for the Al-Mo alloys and from 6 to 15 at.% for the Al-Cr alloys.

Table 1

Variation in Alloy Composition Across the Si Wafer

Alloy	Concentration (at.%)	
	Low	High
Al/Cr	2.8	5.8
Al/Cu	10.5	22.0
Al/Mo	4.0	8.2
Al/Si	1.1	2.1
Al/Ta	4.0	8.8
Al/Zr	2.0	5.5

In addition to the films that were sputter-deposited onto the 2-in.-diam. wafers, several films consisting of pure Al, Al-1.5 Mo, and Al-1.5Cr were deposited onto smaller 16-mm.-diam. wafers. The alloy films were stored in plastic containers that were exposed to the laboratory air. Prior to the onset of the experiments, each surface was analyzed using XPS to obtain the surface chemistry of the air-formed passive film.

Samples used in the electrochemical and XPS studies were made by cleaving the 2-in.-diam. wafer into sections, each of which was attached to a stainless steel holder. The surface of each sample and the holder were coated with a lacquer, leaving an area of approximately 1 cm^2 exposed for polarization, and allowed to dry for 24 h. The coated samples were then exposed to an electrolyte (0.1 M KCl adjusted to pH 8 using KOH), which was mechanically stirred, degassed, and purged with high-purity nitrogen. The samples were polarized anodically at 0.2 mV/s, starting at the open circuit potential (E_{oc}) using a Princeton Applied Research (PAR) Model 273 potentiostat, when the rate of change in E_{oc} was less than 6 mV/h. The electrochemical cell contained a Pt mesh counter-electrode with a surface area at least ten times greater than the working electrode. The potentials were referenced to an external saturated calomel electrode (SCE).

The 16-mm.-diam. samples were mounted into a Teflon holder that had an exposed surface area of 0.95 cm^2 and sealed from the solution with a lacquer-coated Teflon seal that effectively eliminated crevice attack. A setup similar to the above was used to study pit initiation. The samples were allowed to equilibrate in 500 ml of 0.05 N Na_2SO_4 prior to applying a potential of 300 mV(SCE). This potential was chosen because it was significantly above E_b in all of the conditions measured for each alloy: Al, Al-1.5Mo, and Al-1.5Cr. After 600 s, a solution of KCl was injected into the flask, so that the final concentration of the electrolyte was either 0.1 or 0.01 M KCl. The volume of solution injected into the flask was less than 20 ml and had a pH of 8; thus its addition would not substantially perturb the conditions in the flask. The current density was monitored as a function of time, and the

induction period for pit formation (t_p) was noted as a sharp increase in the current density.

Preliminary salt spray (fog) tests were conducted according to ASTM B117-85 "Standard Method of Salt Spray (Fog) Testing" on Al and Al alloys containing from 1-9 at.% of either Cr or Mo. The tests were conducted over a fifty-day period with periodic interruptions to study the extent of the attack. The degree of attack was determined visually; hence, it is a qualitative evaluation.

For the XPS study, a series of polarization experiments was conducted on Al, Al-Mo, and Al-Cr alloys with various solute concentrations and their surface chemistry was subsequently measured. This procedure consisted of polarizing the samples to a set potential, removing them from the electrolyte, rinsing the surfaces with high-purity water and then drying them with nitrogen, removing the lacquer by peeling it off the surface with a scalpel, and transferring them through air into the ultrahigh vacuum (UHV) chamber of the XPS spectrometer. The elapsed time between polarization and insertion into the introduction chamber of the spectrometer was typically less than 6 min. A series of three polarization experiments was performed on the pure Al sample, whereas four experiments were performed on each Al alloy, except for two samples, which were only polarized to -600 mV (SCE) and analyzed. In each series, the same sample was studied to eliminate surface variations between samples and facilitate a study of the change in the chemistry of the passive film as function of applied potential.

The XPS measurements were made using a spectrometer [Surface Science Laboratories (SSL) Model SSX 100-03] with a monochromatized Al Kα X-ray source and a hemispherical electron energy analyzer with multichannel detection. The X-ray source was focussed to a spot size of 600 μm. The sample was isolated from ground during analysis, and the surface charge was neutralized by bombarding the surface with low-energy electrons (~ 2 eV). Each sample was removed from the spectrometer after analysis and stored until the next polarization experiment.

XPS survey spectra were used to obtain a qualitative analysis to ensure that there was no unexpected contamination; high-resolution spectra [with full width at half maximum (FWHM) of the Au $4f_{7/2}$ = 1.1 eV] of the Cr $2p_{3/2}$, O 1s, C 1s, Mo 3d, and Al 2p photoelectron peaks were used for quantitative analysis and chemical state determination. Quantitative analysis was determined from peak areas [using an integral background approximation (13)] and sensitivity factors that were obtained from standards with our spectrometer (11). Chemical state separation was achieved by curve-fitting the data using the manufacturer-provided software. To curve-fit the Mo 3d line lineshape, the two spin-orbit-split components were constrained with an energy separation of 3.2 eV and an area ratio of 1.5. The fits were obtained with the fewest peaks needed, considering all of the data of a given series and the spectral signal-to-noise. The "goodness" of the fits was judged using several criteria: 1) the over-all fit, 2) the fit along the low binding energy edge of the peak, 3) the widths of the individual components (generally, 1.2 to 2.2 eV, with the peaks from the metallic states being narrower than the peaks from the oxide states), and 4) the uniformity of the widths within both the metallic and the oxidized sets of states.

Spectra from several commercially available Mo- and Cr-containing compounds were measured to generate an in-house binding energy data base. In most cases, the samples were powders or small crystallites mounted on double-sided sticky tape. All the samples were kept in the introduction chamber for several hours prior to analysis to remove as much additional water as possible. In addition, several of the compounds were hydroscopic; these were mounted and either loaded into the UHV chamber as quickly as possible or kept in a vacuum dessicator overnight to remove the absorbed water. Although each sample had a thin, oxidized film, curve-fitting facilitated distinguishing the separation between the film and bulk for those samples in which the bulk Mo (Cr) was not in the +6 state.

III. RESULTS

A. POLARIZATION BEHAVIOR

The polarization behavior for each of the alloys is shown in Fig. 1. Each curve in the figure represents a composite of three scans performed on each alloy. The concentration of solute in each alloy differed considerably: pure Al, Al-4.3Cr, Al-15.0Cu, Al-6.1Mo, Al-1.5Si, Al-6.3Ta, Al-3.8Zr. Compared to pure Al, the addition of Si and Zr have little effect on E_{oc}; Ta and Cr additions resulted in more noble potentials for E_{oc}, a shift of approximately 300 mV; and Cu and Mo gave the largest change in E_{oc}, almost 600 mV electropositive shift in potential.

The largest shift in E_b, over 0 mV(SCE), was for the alloy that contained Ta. The addition of Mo to Al also resulted in a substantial electropositive shift. Both the Al-4.3Cr and Al-3.8Zr had similar shifts in E_b, with values closer to -300 mV(SCE). Surprisingly, E_b also became more electropositive for the Al-15Cu alloy. The addition of Si to Al had little impact on the polarization behavior of Al.

B. SALT SPRAY TEST

After 1 day of exposure, the pure Al sample had been heavily attacked, whereas the alloy samples retained their luster and were free from pits. After 7 days of exposure, the pure Al had completely dissolved and only the Si wafer remained; the Al-Mo samples began to turn brown; and the Al-Cr samples retained their luster, with isolated areas of attack in the form of crazing. After 14 days, the Al-Mo samples appeared to be dark brown or black and pits had begun to form on the surface. The Al-Cr samples still retained their luster, although the crazed structure became more well defined at higher Cr levels. The best Al-Cr samples contained only small amounts of Cr (1 at.%). In 30 days, the Si substrate began to appear on the samples containing the lowest concentration of Mo (1-2 at.%). The samples with the highest Mo

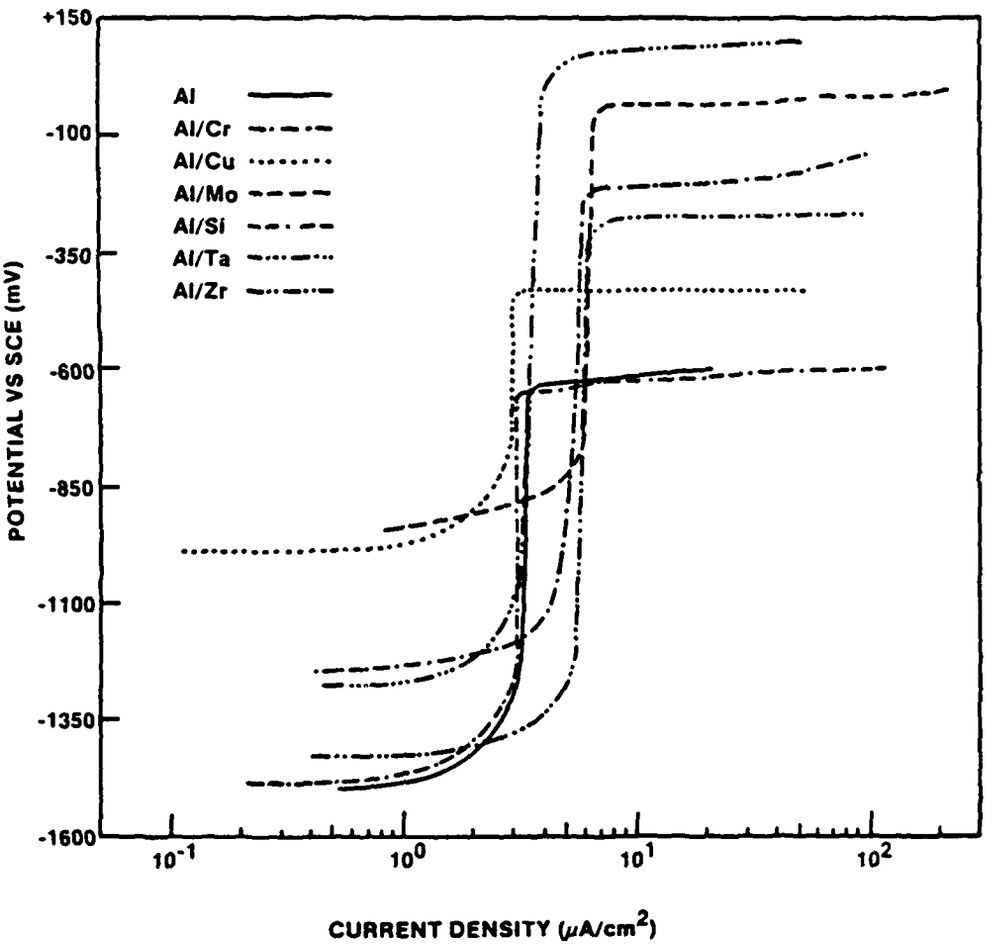

Figure 1. Potentiodynamic polarization curves for pure Al and six different sputter-deposited Al alloys.

concentration (7.0 at.%) were dark and heavily pitted. The Al-Cr samples did not appear to change. After 50 days, all of the Al-Mo samples showed extensive attack. On the other hand, large areas of surface of the Al-Cr samples, particularly those samples with low Cr content, retained a shiny luster. Higher Cr levels led to areas of green discoloration on the surface and pitting only in a few isolated areas.

C. INITIATION TESTS

The results of the pit initiation tests are listed in Table 2. These results indicate that the t_p of Al and Al-1.5Cr differed very little, being well within the experimental scatter. However, the t_p for the Al-Mo alloys increased substantially, indicating a possible change in the mechanism by which pits form in the passive film.

Table 2

Induction Time as a Function of Alloying Addition and Chloride Concentration at 20°C

Alloy	Induction Time, t_p (s)	
	0.01 M KCl	0.1 M KCl
Al	1080	40
Al-Mo	4390	185
Al-Cr	780	25

As the chloride concentration in the solution increases, t_p decreases. Foley and coworkers (14-16) and others (17) have used the functional dependence of the initiation time and the chlorine concentration to estimate n, the number of anions involved at a single surface site during the initial pitting process, by the following rate equation:

$$(1/t_p) = k[Al^{+3}]^m[Cl^-]^n \qquad (1)$$

where k is the rate constant, Al^{+3} and Cl^- are the aluminum and chloride concentrations in the solution, respectively, and m and n are the orders of the reaction. If k, m, and $[Al^{+3}]$ are assumed to be constant, the logarithmic form of this equation results in a linear dependence of the chloride concentration on t_p, with n as the slope of the line. Unlike t_p, the value of n for each alloy is very similar, with n equal to 1.4 for Al and Al-1.5Mo, and 1.5 for Al-1.5Cr. This result suggests that the same species initially form on the surface in each of the alloys during the onset of the pitting process.

D. PASSIVE FILM CHEMISTRY

D1. Binding Energy Standards

Two alloying additions, Mo and Cr, were studied in detail to help eludicate the mechanism by which the presence of the element in the passive film inhibits pit formation.

Interpreting XPS spectra often becomes complex as the number of possible oxidation states increases. To resolve the chemical species that may be present, we analyzed a number of different Mo- and Cr-containing compounds to help identify differences in oxidation states (see Table 3). Spectra were obtained from nearly all compounds at least twice. The typical deviation in binding energies was 0.2 eV or less, indicating good precision in the values quoted. In addition to these data, several other sources were used as references (7,8,18-28). The results listed in Table 3 show good agreement between the current results and those in the literature. These results indicate that the Mo^{+4}- and Mo^{+6}-containing compounds exhibit a variation in binding energies of approximately 1 eV. The binding energy of the molybdate compounds is cation dependent. Furthermore, Olefjord et al. (7) indicated that the binding energy of Mo^{+4}-containing compounds depends strongly on the Mo coordination. For example, the binding energy for MoO_2 is 1.6 eV lower than for a hydrated

Table 3

Binding energy for Mo and Cr Metal and Compounds

Oxidation State	Compound	Binding Energy (eV) This work [a]	Other work	Ref.
		Molybdenum		
0	Mo metal	227.9	227.4 [b]	18
			228.0 [a]	19
			227.7 [a]	20
			227.8 [b]	21
			227.7 [a]	7
+2	Mo_2C	228.6		
+3	$MoCl_3$	230.0	229.7 [a]	20
			229.7 [a]	8
+4	MoO_2	229.5	229.2 [b]	18
			229.4 [a]	19
			229.4 [a]	20
			229.3 [a]	7
			229.4 [b]	22
	Mo^{hy}		230.9 [a]	7
			230.2 [a]	8
	MoS_2	229.8	228.9 [a]	20, 22
			228.9 [b]	18
	$MoCl_4$	230.4	230.4 [a]	20
+5	$MoCl_5$	232.2	230.7 [a]	20
	Mo_2O_5		231.4 [b]	21
+6	$CoMoO_4$		231.8 [b]	20, 22
	Na_2MoO_4	231.8	232.1 [a]	20
	MoO_2Cl_2 [c]	232.6		
	$Al_2(MoO_4)_3$	232.8	232.7 [a]	20
	MoO_3	232.9	232.4 [b]	20
			232.5 [a]	19
			232.6 [a]	20
			232.2 [b]	21
			232.5 [a]	7
			232.5 [b]	8
	$MoOCl_4$ [c]	233.0		

Table 3 (cont.)

		Chromium		
0	Cr metal	573.8	574.0 [a]	23
			574.2 [b]	24
			574.4 [a]	7
			574.1 [a]	25
			574.1 [a]	20
			573.87[b]	26
+3	Cr_2O_3		576.2 [a]	23
			576.0 [a]	7
			576.3 [a]	25
			576.6 [a]	20
			576.25[b]	26
			576.6 [a]	28
	CrOOH		576.6 [a]	23
			577.0 [a]	25
			576.8 [a]	20
			576.8 [b]	27
			577.2 [a]	28
	$Cr(OH)_3$		577.7 [a]	7
			577.0 [a]	25
			577.4 [a]	20
			576.76[b]	26
	$CrCi_3$		577.2 [a]	20
			577.6 [a]	20
+4	CrO_2		576.1 [a]	20
			576.1 [b]	27
+6	CrO_3	579.0	577.7 [a]	23
			578.1 [a]	25
			578.1 [a]	20
			579.07[b]	26
	$BaCrO_4$		578.9 [a]	20
	K_2CrO_4	578.8	579.4 [a]	20
	$K_2Cr_2O_7$	579.0	579.3 [a]	20
			579.6 [b]	27

[a] Referenced to C 1s at 284.6 eV.
[b] Referenced to Au $4f_{7/2}$ at 83.8 eV.
[c] Surfaces were deficient in Cl and may have decomposed.

form Mo^{hy}. Nevertheless, each state (except for Mo^{+3} and Mo^{+4} and, possibly, Mo^{+5} and Mo^{+6}) has a distinct set of binding energies. The Cr^{+3}- and Cr^{+6}-containing compounds also have ranges in binding energy, but again, the ranges are distinct and allow assignment of the different oxidation states.

D2. Sample Transfer

XPS measurements are by necessity ex situ. Consequently, any changes in the chemistry of the passive film caused by removing the sample from the electrolyte and transferring it through the air to the UHV chamber must be characterized. Earlier work on pure Al showed that the transfer of the sample over short times, i.e., approximately five minutes, had very little effect on the chemistry of the passive film that had been formed in dilute sodium sulfate solutions (12). Exposure of the passive film to the UHV environment resulted in the removal of adsorbed water from the film, without changing its chemistry from the oxyhydroxide phase.

The effect of air transfer may become more important for Al alloys containing Mo, because some of the hydrated Mo compounds that might exist in the film are unstable in air (29). To address this problem, several experiments were performed on the transfer of Al samples that had been exposed to solutions containing low concentrations of molybdates (10 ppm), which results in an Al surface containing a high concentration of Mo^{+4} in the passive film (26). This surface component would be the one that is most sensitive to air oxidation. These samples were either exposed to air for various lengths of time or transferred to the UHV chamber under an argon cover gas. The results of these experiments indicate that for our transfer cycle, which ranges between 3-6 min, no detectable changes occurred in the film.

D3. Passive Film Characterization Using XPS

The electrochemical potentials for each sample, including the initial E_{OC} measurement and the final applied potential, are listed in Table 4. In the first experiment, the sample is allowed to come to equilibrium and is then

removed for analysis; therefore, only the E_{oc} value is given. In subsequent experiments, the sample was polarized, and the final potential is also listed. The consistency of the E_{oc} for the sample for each experiment is strong evidence that no irreversible changes occur during the transfer, measurement, and storage procedure. Samples AM-4 and AC-4 were used in a separate study involving variable take-off angle XPS to help elucidate the structure of the film. These were polarized only once up to -600 mV(SCE).

Table 4

Polarization Experiments of the Binary Aluminum Alloys in Deaerated 0.1 N KCl Adjusted to pH 8

			Experiment Number 1	2	3	4
Sample	Conc. (at.%) Mo	Cr	E_{oc} [mV(SCE)]	E_{oc}/E_{final} [mV(SCE)]	E_{oc}/E_{final} [mV(SCE)]	E_{oc}/E_b [mV(SCE)]
Al	--	--	-1511	-1491/-900	----	-1514/-442
AM-1	2.2	--	-1046	-1039/-600	-1003/-400	-978/-325
AM-2	7.8	--	-888	-893/-600	-894/-400	-931/ -4
AM-3	12.0	--	-950	-930/-600	-891/-400	-879/+250
AM-4	16.0	--	----	-912/-600	-----	----
AC-1	--	6.8	-1125	-1107/-600	-1099/-400	-1137/-232
AC-2	--	8.0	-1128	-1122/-600	-1107/-400	-1156/-202
AC-3	--	14.0	-1026	-1000/-600	-1021/-400	-977/-247
AC-4	--	15.0	----	-1047/-600	----	----

The addition of both Mo and Cr to Al resulted in an increase in the E_{oc}; however, the E_{oc} of the Al-Mo alloy increases with higher solute concentrations, whereas the E_{oc} of the Al-Cr alloys is less dependent upon the solute concentration. E_b shows a similar trend, increasing dramatically for

the Al-Mo alloys, but remaining independent of concentration for the Al-Cr alloys. These results on the Al-Mo alloys agree with our earlier work (3,4).

The surface chemistry was studied using XPS as a function of applied potential. Initially, the surface is covered with a thin, air-formed oxide film. The area ratio of Al^0/Al^{+3} ranges between 0.3 to 0.4 for Al and each alloy, which corresponds to an oxide thickness of ~ 3.5 nm. Metallic Mo or Cr is also detectable in the alloy surface. The Mo in the air-formed film of AM-1 appears as Mo^{+4} (229.8 eV), which corresponds closely to MoO_2. No oxidized Mo or Cr was detected in any of the other samples at this stage. Our work also shows the presence of a state that has a lower binding energy than the elemental Mo (Mo^{el}) or Cr (Cr^{el}) states, which have binding energies at 227.3 eV and 574.0 eV, respectively. We attribute the state at the lower binding energy (225.8 eV for Mo and 572.2 eV for Cr) to the presence of the solute in the alloy (Mo^{al} or Cr^{al}), i.e., Mo or Cr in an Al environment. Although the shift (1.5 eV or 1.8 eV) is larger than has been reported for most alloy systems (31,32), results from variable take-off angle XPS discussed later in this section indicate that the Cr^{el} and Mo^{el} reside at the metal/film interface, which supports this conclusion.

Exposing the sample to the electrolyte causes the surface to oxidize and increase in thickness. The ratio of Al^0/Al^{+3} drops to 0.13 for pure Al (~ 6.0 nm). In the Mo-containing alloys, the decrease in the Al^0/Al^{+3} ratio is even greater, falling to as low as 0.02 (~ 80 nm). On the other hand, the Al^0/Al^{+3} ratio only decreases to 0.2 (~ 45 nm) for the Al-Cr alloys, indicating that the film formed on the Al-Mo alloys is thicker than that formed on either the Al or the Al-Cr alloy samples.

Exposing the sample to the electrolyte at E_{oc} results in higher oxidation states of the solute species in the passive film. The peak due to the metallic state is also still present, although diminished. The Al-Mo alloy shows the Mo^{+6} state (232.2 eV) as well as two separate species, with lower binding energies, the first at 228.7 - 229.2 eV and the second at 230.6 eV.

The higher binding energy at 230.6 eV is assigned to the hydrated Mo^{+4} state (7). The remaining oxidation state exhibits a binding energy shift during polarization. It appears at 228.7 eV at low overpotentials and increases to 229.2 eV at higher overpotentials. We identify the higher binding energy peak as MoO_2 and tentatively attribute the peak at 228.7 eV to an intermediate state, designated as Mo^{in}, during the oxidation of Mo in the alloy. Figure 2 shows the presence of Mo and the other states of Mo on the surface of AM-2 as a function of applied potential. In all three samples, no one oxidation state is dominant in the passive film, and the concentration of each oxidation state in the passive film increases for each alloy as the bulk alloy concentration increases (see Table 5).

Table 5

Contribution of Solute Species to the Passive Film for the Al-Mo Alloys

	Concentration (at.%)[a]						
	Mo^{al}	Mo^{el}	MoO_2/Mo^{in}	Mo^{hy}	MoO_4^{-2}	Al^0	Al^{+3}
AM-1							
As-dep.	0.24	0.05	0.05	--	--	11.11	28.8
E_{oc}	0.14	0.07	0.29	0.07	--	0.72	31.1
-600	--	--	1.37	0.68	1.13	--	28.4
-400	--	--	0.22	1.17	0.46	--	26.2
-325	--	--	--	1.00	0.27	--	26.8
AM-2							
As-dep.	0.73	0.11	--	--	--	11.95	31.0
E_{oc}	0.44	0.44	0.23	0.28	--	2.83	38.2
-600	0.07	0.40	1.50	1.12	0.58	0.58	34.4
-400	--	--	1.19	2.29	1.13	--	29.7
-4	--	--	1.03	2.08	1.03	--	27.2
AM-3							
As-dep.	0.82	--	--	--	--	9.06	28.2
E_{oc}	0.37	0.28	0.23	0.32	--	2.23	33.2
-600	--	0.26	2.66	1.95	3.04	--	20.0
-400	--	--	0.35	3.34	2.06	--	24.0
+250	--	--	0.21	4.21	0.88	--	25.9

[a] Adventitious C and the O associated with it have been excluded from the concentration normalization

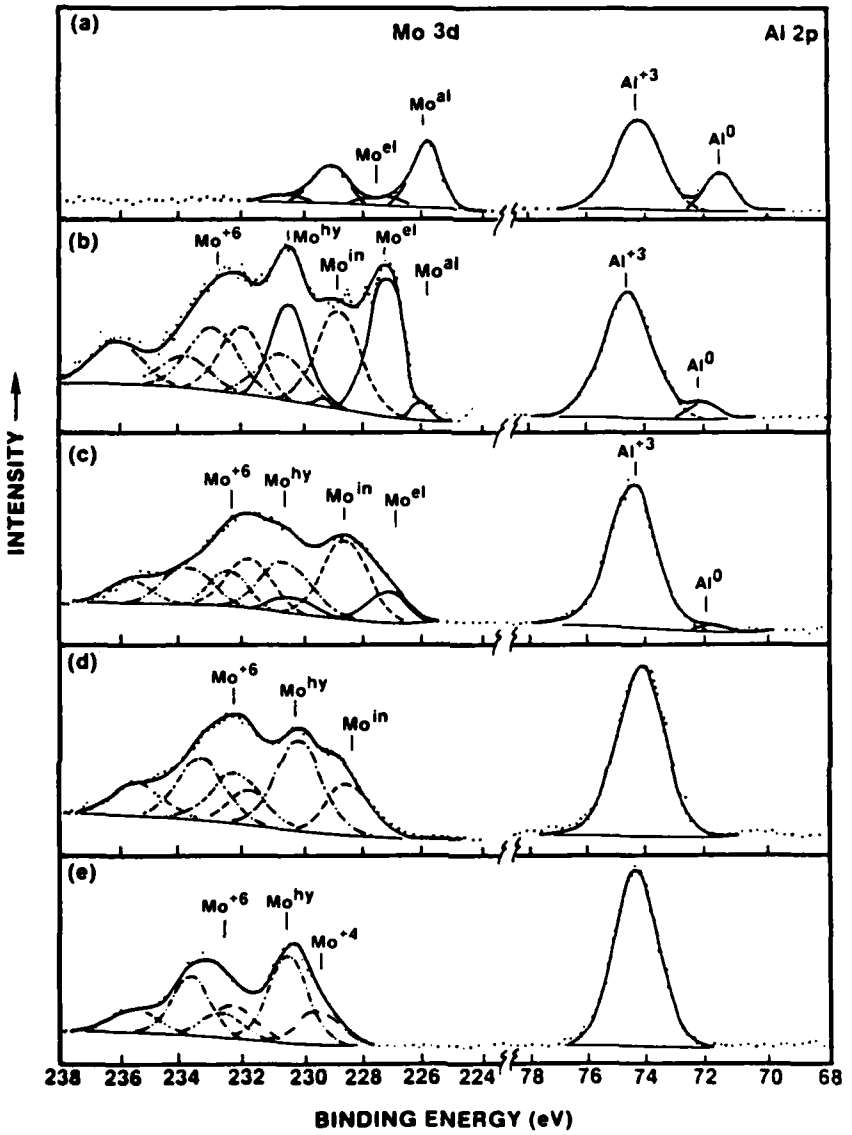

Figure 2. Variation of the Al 2p and Mo 3d spectra as a function of applied potential for sample AM-2 (Al-7.8Mo): a) As-sputter-deposited, b) at E_{oc} [-931 mV(SCE)], c) at -600 mV(SCE), d) at -400 mV(SCE), and e) at E_b [-4 mV(SCE)].

The Al-Cr alloys also show a multiple number of states in the surface region when exposed to the electrolyte at open circuit conditions (Table 6); however, the concentration of Cr in the oxide is independent of the bulk alloy concentration. In addition, the Cr^{+3} state [at 576.9 eV, corresponding to either the trihydroxide phase, $Cr(OH_3)$, or the Cr oxyhydroxide phase, CrOOH] is the dominant oxidation state in the passive film, although the Cr^0 peaks are still present. The ratio of Cr^0/Al^0 (Cr^0 includes both the peak at 572.2 eV, Cr^{al}, and that at 574.0 eV, Cr^{el}) increases at the open circuit potential from the value found in the air-formed passive film, indicating that Cr is building up at the metal/film interface. This suggests that Al is being preferentially increased with oxide thickness, thereby indicating that a layer of Cr^{el} is forming under the passive film.

Polarizing the Al and the binary alloys results in a continued oxidation of the surface and thickening of the passive film. For Al polarized to -900 mV(SCE) and the Al-Mo alloys polarized to -600 mV(SCE), approximately a 500 mV overpotential, the contributions of the metallic Al and Mo signals are not detected. The Al-Cr alloys, on the other hand, still have a small signal coming from the metallic Al state. Figure 3 shows the Al and Cr spectra from AC-1 as a function of applied potential.

Greater electropositive potentials above E_{oc} initially lead to an increase in the Mo^{ox} (oxidized Mo) signal, followed eventually by a decrease in the concentrations of Mo in the passive film. Furthermore, the Mo^{ox}/Al^{ox} (oxidized Al) ratio in the film increases as a function of the bulk alloy composition. Figure 4 and Table 5 show the trend of oxidized Mo in the film as a function of applied potential. In AM-2 and AM-3, three chemical species are present, whereas only two are detectable for AM-1. As the applied potential is increased, the contribution of the Mo signal due to the Mo^{+6} state decreases, and the dominant oxidation state becomes the Mo^{hy} at a binding energy of 230.6 eV, indicating that the Mo in the film is hydrating during polarization up to more noble potentials. The contribution of the Mo signal

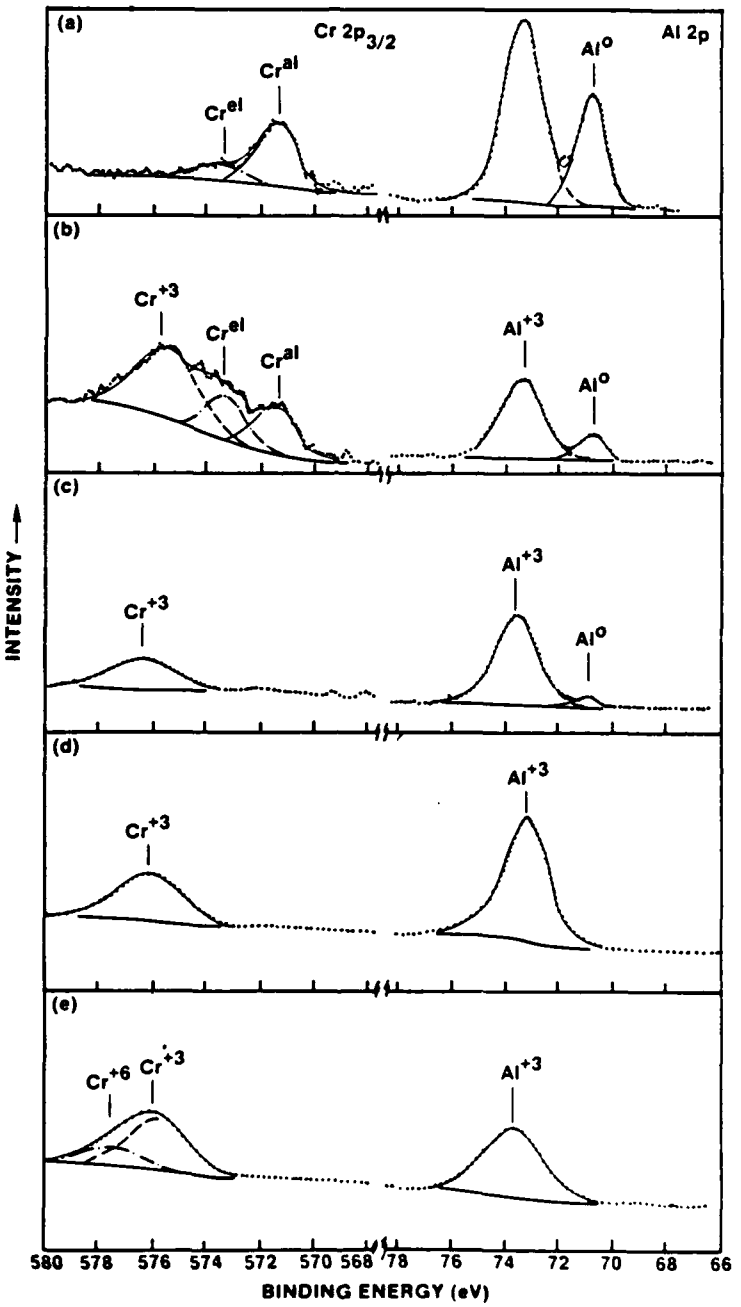

Figure 3. Variation of the Al 2p and Cr $2p_{3/2}$ spectra as a function of applied potential for sample AC-1 (Al-6.8Cr): a) As-sputter-deposited, b) at E_{OC} [-1125 mV(SCE)], c) at -600 mV(SCE), d) at -400 mV(SCE), and e) at E_b [-232 mV(SCE)].

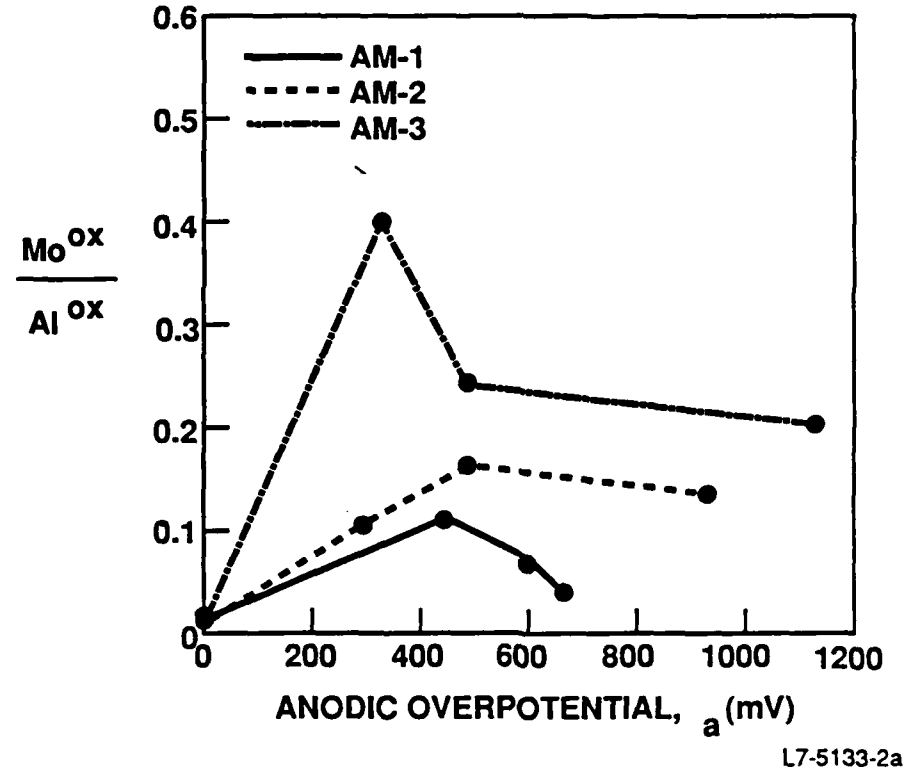

Figure 4. The Mo^{ox}-to-Al^{ox} ratio as a function of anodic overpotential.

Table 6

Contribution of Solute Species to the Passive Film for the Al-Cr alloys

	Concentration (at.%)[a]						
	Cr^{al}	Cr^{el}	$Cr(OH)_3$	Cr_2O_3	CrO_3	Al^0	Al^{+3}
AC-1							
As-dep.	0.69	0.21	--	--	--	12.70	30.8
E_{oc}	0.48	0.43	--	1.11	--	5.25	31.7
-600	--	--	3.70	--	--	1.30	30.3
-400	--	--	5.70	--	--	--	27.8
-232	--	--	8.90	--	2.20	--	22.4
AC-2							
As-dep.	0.66	0.20	--	--	--	13.23	29.3
E_{oc}	0.33	0.24	1.75	--	--	4.50	29.7
-600	--	--	2.00	--	--	2.90	30.0
-400	--	--	8.80	--	--	--	19.4
-202	--	--	6.45	--	3.50	--	17.0
AC-3							
As-dep.	0.82	0.27	--	--	--	12.41	33.3
E_{oc}	0.77	0.22	0.58	--	--	4.50	32.3
-600	0.70	0.60	2.60	--	0.80	1.80	30.1
-400	--	0.80	4.10	1.00	1.10	--	29.7
-247	--	--	6.00	1.30	3.70	--	20.7

[a] Adventitious C and the O associated with it have been excluded from the concentration normalization.

at 230.6 eV increases from 20% of the total Mo^{ox} signal in each alloy at E_{oc} to 80% at E_b. In contrast, the contribution of the Mo^{+6} state at 232.2 eV increases at -600 mV(SCE) compared to that at E_{oc}, but subsequently falls off as the potential becomes more noble.

The behavior of Cr in the passive film is quite different from Mo. The concentration of Cr in the film increases with applied potential; it does not appear to be strongly tied to the bulk Cr concentration. For AC-1 and AC-2,

only the Cr^{+3} [$Cr(OH)_3$ or CrOOH] is present above -600 mV(SCE) up to E_b. At E_b, the Cr^{+6} state appears. For AC-3, the Cr^0, Cr^{+3} [both Cr_2O_3 and $Cr(OH)_3$ or CrOOH], and the Cr^{+6} (CrO_3) states are present up to -400 mV(SCE). However, in all cases, the Cr^{+3} state [$Cr(OH)_3$ or CrOOH] is the dominant state in the passive film (Table 6). At E_b, all three films contain a significant amount of Cr^{+6}, which increases as a function of the bulk alloy concentration.

The concentration of Cr in the passive film relative to the Al increases monotonically as a function of applied potential (Fig. 5). The ratio of Cr^{ox}(oxidized Cr)/Al^{ox} increases to between 0.4 to 0.6 at the breakdown potential. The concentration of Al^{ox} in the passive film decreases to as low as 17 at.% in AC-1 at Eb, compared to 27 at.% for the Al-Mo alloys and 32 at.% for pure Al.

Variable take-off angle XPS was used to study the structure of the film that forms at -600 mV(SCE) on two solute-rich samples, AM-4 and AC-4. The take-off angle of the photoelectrons was varied from the standard 38° (relative to the surface) to near glancing. Because photoelectrons from a given depth emitted at low angles traverse more material than those emitted at higher angles, they are attenuated to a greater degree. Thus, measurements taken at near glancing angles are more surface-sensitive. The results shown in Table 7 were acquired at glancing and standard conditions. The first two columns contain data for which the adventitious carbon on the surface has been taken into consideration in determining surface concentrations. In the second set of columns, adventitious carbon and the oxygen associated with it have been removed. As expected, C is found at the film surface. The amount of C drops considerably going from the glancing to the standard angle, whereas the oxygen signal increases. This result is expected, since the carbon occurs as a result of exposing the sample to the atmosphere. Once the carbon and excess oxygen signals have been removed, the passive film can be analyzed. In the case of AM-4, there is little variation of the chemistry as a function of depth. Slightly more oxidized Al appears at the surface; however, both the

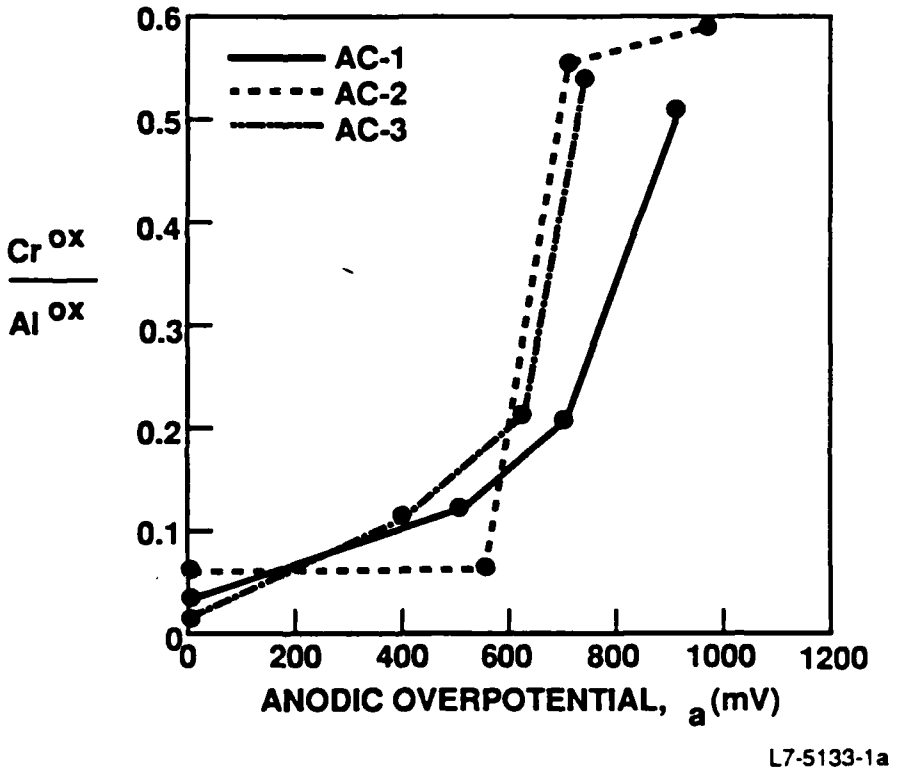

Figure 5. The Cr^{ox}-to-Al^{ox} ratio as a function of anodic overpotential.

MoO_2 and MoO_4^{-2} seem to be evenly distributed throughout the film, and no Mo^{hy} was detected. An important feature of this table is that Mo^{el} appears closer to the surface than Mo^{al}, indicating that Al is preferentially oxidized and leaves behind a Mo-rich layer between the alloy and the passive film. It further confirms our conclusions that the binding energy of Mo in the alloy is substantially shifted away from the binding energy of elemental Mo.

Table 7

Variations in the Surface Chemistry of AM-4 and AC-4 after Polarization up to -600 mV(SCE) as a Function of Take-off Angle

	As-Detected		Carbon-Corrected	
	Glancing	Standard	Glancing	Standard
		Aluminum-Molybdenum		
Al^{+3}	6.9	12.2	29.7	26.7
Al^0	--	0.5	--	1.2
Mo^{el}	0.02	0.09	0.09	0.20
Mo^{al}	--	0.10	--	0.22
$Mo^{+4}(MoO_2)$	0.05	0.10	0.21	0.22
$Mo^{+6}(MoO_4^{-2})$	0.06	0.13	0.26	0.28
C	65.8	49.2	--	--
O	27.2	37.6	69.8	71.3
		Aluminum-Chromium		
Al^{+3}	1.9	6.4	9.5	21.5
Al^0	--	1.1	--	3.6
Cr^{el}	--	0.08	--	0.27
Cr^{al}	--	0.20	--	0.68
$Cr^{+3}(Cr_2O_3)$	0.23	0.33	1.1	1.1
$Cr^{+3}[Cr(OH)_3]$	0.16	0.55	0.8	1.9
C	72.7	60.5	--	--
O	24.9	30.9	88.6	71.0

Compared to AM-4, the variation in data for AC-4 as a function of take-off angle shows quite different features. The level of Al in the film decreases from the metal/film interface to the surface and the AC-4 film is thinner and contains substantially more Al^0 at the standard take-off angle. The Cr_2O_3 that forms in the film for the Al-Cr alloys with high solute content is present throughout the film and, like the MoO_2 and MoO_4^{-2} that form in the AM-4 film, does not vary in concentration as a function of depth. In contrast, the $Cr(OH)_3$ phase does vary and appears to reside closer to the metal/film interface. The amount of oxygen in the film is high, indicating that even at this potential, the area closest to the film/solution interface contains a high number of cation vacancies. The ratio of metal oxide-to-oxygen in the film at the standard take-off angle is 0.35, and decreases to 0.13 at the surface, indicating that the surface region is oxygen rich. In comparison, the metal oxide-to-oxygen ratio for the AM-4 films is 0.38 at the standard take-off angle, and remains constant throughout the film, increasing only slightly to 0.43 at the glancing take-off angle.

Although the films that form on AM-4 and AC-4 differ greatly, both samples form a metal-rich region between the passive film and the alloy. As in the AM-4 sample discussed earlier, two metallic states appear for the Al-Cr alloys. One state is associated with Cr in the alloy, and one with Cr metal. The Cr^{al} and Cr^{el} appear only at the standard takeoff angle, indicating that they reside beneath the passive film.

IV. DISCUSSION

The addition of the different alloying additions to aluminum generally resulted in more noble E_b. The addition of Ta resulted in the largest change in pitting potential, with Mo, Cr, and Zr also showing a substantial increase in E_b. Although each of the elements had an impact on the corrosion behavior of the alloy in the electrolyte, further investigation of the passive film on

Al, Al-Cr, and Al-Mo alloys show that the mechanism by which passivation occurs can be very different.

The results of the salt spray study indicate that Cr readily protects Al against attack in oxidizing chloride-rich environments. In contrast, Mo does not protect the Al from general attack or hydration, as evidenced by the change in color of the film, although it does increase the breakdown potential.

The time needed to nucleate a pit in the Al-1.5 Mo was almost an order of magnitude longer than that for either the Al-1.5 Cr or pure Al samples. This may be due to the thickening of the film in the presence of Mo or to the strong effect that the Mo^{+6} state has on the entry of Cl^- into the film. However, the values for the order of reaction suggest that the chemistry of pit formation proceeds in a similar fashion for each alloy, independent of the solute addition. The value for the order of the reaction is similar to values obtained on Al and Al alloys by Foley (14). Hence, the actual breakdown of the film is still dependent upon the interaction of Al in the film and Cl^- anion in the solution.

A study of the passive film as a function of applied potential using XPS indicates that its composition and thickness change as the potential approaches E_b. Thickness increases at higher anodic potentials, and Mo and Cr are incorporated in the film during polarization. The changes in the film of each alloy coincides with a more noble E_b and indicates that the solute profoundly affects the alloys' corrosion characteristics.

Examination of the film at E_{oc} and -600 mV(SCE) for the alloys and -900 mV(SCE) for pure Al reveals that its thickness varies significantly. The growth of the passive film on Al has been shown to be diffusion of anions, i.e., oxygen, through the film to the metal/film interface (29). Thus, Mo and Cr seem to affect the film in different ways. For the Al-Mo alloys and pure Al, the film thickens relatively quickly, and at -600 mV(SCE) is substantially thicker than the alloys containing Cr at approximately the same overpotential. The solute builds up at the metal/film interface for both the Al-Mo and Al-Cr

alloys, indicating that Al is more easily oxidized than either solute, although the buildup at the interface is more pronounced with the Cr-containing alloys.

The differences in film thickness between the alloys suggest that a number of mechanisms might be active. The Cr either 1) impedes the movement of oxygen anions through the film, 2) limits the formation of cations at the metal/film interface, or 3) increases the rate at which cations leave the film and enter the solution. Several factors indicate that the Cr in the alloy does not impede the diffusion of Al cations or oxygen anions through the passive film during film growth. As the applied potential is increased, the ratio of Cr^{ox}/Al^{ox} also increases. The increase is the result of a loss of Al^{ox} in the film, indicating that the Al is dissolving preferentially. Furthermore, at -400 mV(SCE), the signal due to the metallic Cr peak is still detectable on AC-3, whereas the signal due to the metallic Al peak has vanished. (For AM-3, neither the Al^0 nor the Mo^0 peaks are detectable.) Although the XPS measurements are much more sensitive to Cr than Al (15:1), the ratio of Cr/Al in the alloy (1:8) is such that if the metal peaks are in a constant stoichiometric mixture, they should become indistinguishable from the background-induced noise at approximately the same oxide thickness. The presence of the Cr-rich region at the metal/film interface and the loss of Al from the film indicates that Al is preferentially oxidized at the metal/film interface, and a sufficient supply of oxygen anions are present at the metal/film interface to react with the Al. Therefore, cations must be leaving the film faster than they are being replaced, indicating that film growth for the Al-Cr alloys is limited by the supply of readily oxidizable Al, as indicated by the depletion of Al from the film, and not by the diffusion of oxygen anions to the metal/film interface.

The inhibition of Al oxidation at the metal/film interface indicates that a barrier has formed in this region. This barrier layer consists primarily of Cr^{+3} [$Cr(OH)_3$ or CrOOH], which is the dominant oxidation state of Cr

in the film. At higher potentials and alloy concentrations, Cr^{+6} (CrO_3) is also detected. (The Cr_2O_3 also exists in the film in AC-3.) The coexistence of both Cr_2O_3 and CrO_3 in passive films has been reported for Fe-Cr alloys (9), and is due to the similar value of the standard free enthalpies of the two compounds (34). According to our results, an analogous behavior exists in the passive film of Al-Cr alloys.

The presence of chromium hydroxide at the metal/film interface appears to restrict the oxidation of Al in AC-1 and AC-2, since no other Cr oxidation state is detected in the film below E_b. As the potential approaches E_b, the ratio of $CrO_3/Cr(OH)_3$ increases, indicating that the Cr oxidation reaction is being driven toward the more highly oxidized Cr^{+6} species. The protective nature of the barrier layer breaks down when a significant fraction of the Cr^{ox} is present as Cr^{+6}. This indicates that the barrier is oxidizing and can no longer protect the underlying alloy from oxidation. Unlike the chromium hydroxide film, which is stable in aqueous environments, the chromium trioxide is soluble, and will not serve as a protective film.

The addition of Mo to Al results in a thicker film relative to the Al-Cr alloys, suggesting that Mo in the oxide does not impede the oxidation reaction of the Al. The Mo in the film has been oxidized to a number of different states. As the potential approaches E_b, the contribution of the Mo^{ox} signal due to Mo^{hy} increases, while both Mo^{+4} (MoO_2 or Mo^{in} in the case of AM-2) and Mo^{+6} (MoO_4^{-2}) diminish. At E_b, Mo^{+4} contributes 1%, and Mo^{+6} less than 10%, of the Mo^{ox} signal. The increase of Mo^{hy} in the film at potentials up to E_b suggests that the outer surface is reacting with OH^- ions to form a hydrated film. This region does not appear to protect the alloy from attack by the Cl^- anion, since pitting occurs when the concentration of this phase in the film is large. The MoO_4^{-2} on the other hand, decreases at more noble potentials. We would expect the presence of a stable molybdate anion in the film in this region to impede the movement of anions, thereby protecting the underlying alloy from attack. At higher Mo concentrations, more Mo is found in the oxide

and the molybdate layer is found at higher potentials. This result correlates the shift in E_b with the presence of MoO_4^{-2} in the passive film.

Although the binding energy of the Mo^{+6} state appears to indicate that the passive film contains molybdate anions, the structure of the molybdate is not clear. Table 3 indicates that the binding energy for $Al_2(MoO_4)_3$ is 1 eV higher than the binding energy determined from the peak fit. The binding energy of the Mo 3d spectrum from the passive film is closer to Na_2MoO_4; however, no cations other than Al are present in the spectra. This indicates that the Mo^{+6} may be incorporated into the Al oxide lattice with a more complex local chemistry and structure than a stoichiometric compound such as $Al_2(MoO_4)_3$.

The XPS results indicate that the mechanism by which E_b is shifted to more noble potentials differs for the Al-Cr and Al-Mo alloys. The Al-Cr alloys form a barrier that impedes oxidation but as the potential increases, Al continues to leave the film whereas Cr remains at the barrier layer. Breakdown occurs when the potential reaches a point that favors the sufficient formation of the less protective CrO_3 rather than $Cr(OH)_3$. The breakdown potential remains independent of the alloy concentration because the breakdown of the chromium hydroxide layer is a result of the preferential formation of CrO_3.

In contrast, the Al-Mo alloys form a multilayer film that contains hydrated Mo, concentrated in the outer region, and a molybdate compound concentrated in the inner region. Unlike the Al-Cr alloys, the Mo does not control the oxidation of Al at the metal/film interface and its concentration in the film increases with its amount in the alloy. As the potential is increased, the amount of Mo^{+6} in the film decreases, and the hydrated Mo compound dominates the film. Eventually, the hydration of the film is driven to the extent that the molybdate concentration becomes severely depleted, and Cl^- anions reach the metal/film interface, resulting in breakdown. The breakdown potential is a function of the concentration Mo^{+6} in the film, which

increases with the bulk alloy concentration. Therefore, E_b is a function of the Mo in the alloy.

The results of the XPS work suggest that the mechanism by which pitting on Al-Cr and Al-Mo alloys occurs is different. This correlates with the change in the time to initiate a pit in various concentrations of Cl^- (Table 2) as well as with the salt spray test results.

IV. CONCLUSIONS

The addition of Mo or Cr to Al results in driving E_b to more noble potentials. However, the mechanism by which pits nucleate in the two alloys are quite different. Whereas Mo forms a protective molybdate layer that restricts the movement of Cl^- anions, Cr forms a barrier layer that impedes Al oxidation and inhibits the ingress of anions to the alloy.

The salt spray test showed that Mo did not protect the surface from corrosion or hydration attack. However, Cr was more successful in resisting hydration. This may be due to the fact that although Mo forms a highly charged film that impedes Cl^- movement, it does not stop the growth of the film, and hence, hydration. In contrast, Cr forms a barrier that inhibits movement of both Al into the film and anions from the film to the substrate, thereby protecting the film from hydration.

VI. ACKNOWLEDGMENTS

The authors gratefully acknowledge the sputter-deposition work of Dr. Scott Duncan and Jim Slunt. In addition, the authors would like to thank Dr. A.J. Sedriks for his support.

VII. REFERENCES

1. A.H. Al-Saffer, V. Ashworth, A.K.O. Bairamov, D.J. Chivers, W.A. Grant, and R.P.M. Procter, Corros. Sci., 20, 127 (1980).

2. P.M. Natishan, E. McCafferty, and G.K. Hubler, J. Electrochem. Soc., 133, 1061 (1986).

3. W.C. Moshier, G.D. Davis, J.S. Ahearn, and H.F. Hough, J. Electrochem. Soc., 133, 1063 (1986).

4. W.C. Moshier, G.D. Davis, J.S. Ahearn, and H.F. Hough, J. Electrochem. Soc., 8, 2677 (1987).

5. J.E. Castle, Surf. Interface Anal., 9, 345 (1986).

6. N.S. McIntyre, in "Practical Surface Analysis," D. Briggs and M.P. Seah, Editors, p. 397, Wiley, Chichester (1983).

7. I. Olefjord, B. Brox, and U. Jelvestam, J. Electrochem. Soc., 132, 2854 (1985).

8. C.R. Clayton and Y.C. Lu, J. Electrochem. Soc., 133, 2465 (1986).

9. A.R. Brooks, C.R. Clayton, K. Doss, and Y.C. Lu, J. Electrochem. Soc., 133, 2459 (1986).

10. J. Augustynski, in "Passivity of Metals," R.P. Frankenthal and J. Kruger, Editors, p. 989, Electrochemical Society, Princeton, N.J. (1978).

11. G.D. Davis, W.C. Moshier, J.S. Ahearn, H.F. Hough, and G.O. Cote, J. Vac. Sci. Technol., A 5, 1152 (1987).

12. W.C. Moshier, G.D. Davis, and J.S. Ahearn, Corros. Sci, 27 (8), 785 (1987).

13. D.A. Shirley, Phys. Rev, B 5, 4709 (1972).

14. R.J. Foley, Corrosion, 42(5), 277 (1986).

15. T.H. Nguyen and R.T. Foley, J. Electrochem. Soc., 126(11), 1855 (1979).

16. S. Dallek and R.T. Foley, J. Electrochem. Soc., 122(10), 1296 (1976).

17. Z.A. Forousis and M.J. Thubrikar, J. Electrochem. Soc., 122(10), 1296 (1975).

18. D.S. Zingg, L.E. Makovsky, R.E. Tischer, F.R. Brown, and D.M. Hercules, J. Phys. Chem., 84, 2898 (1980).

19. T.H. Fleisch and G.J. Mains, J. Chem Phys., 76, 780 (1982).

20. C.D. Wagner, W.M. Riggs, L.E. Davis, J.F. Moulder, and G.E. Muilenberg, "Handbook of X-ray Photoelectron Spectroscopy," Perkin-Elmer, Eden Prairie, MN (1979).

21. T.L. Barr, J. Phys. Chem., 82, 1801 (1978).

22. T.A. Patterson, J.C. Carver, D.E. Leyden, and D.M. Hercules, J. Phys. Chem., 80, 1700 (1976).

23. R.W. Bigelow, J.G. Black, C.B. Duke, W.R. Salaneck, and H.R. Thomas, Thin Solid Films, 94, 233 (1982).

24. H.J. Mathieu and D. Landolt, Corros. Sci., 26, 547 (1986).

25. A.R. Brooks, C.R. Clayton, K. Doss, and Y.C. Lu, J. Electrochem. Soc., 133, 2459 (1986).

26. K. Asami and K. Hashimoto, Corros. Sci., 17, 559 (1977).

27. I. Ikemoto, K. Ishii, S. Kinoshita, H. Kuroda, M.A.A. Franco, and J.M. Thomas, J. Solid State Chem., 17, 425 (1976).

28. J.C. Carver, G.K. Schweitzer, and T.A. Carlson, J. Chem. Phys., 57, 973 (1972).

29. M. Pourbaix, in "Atlas of Electrochemical Equilibria in Aqueous Solutions," p. 278, Pergamon Press Ltd., Oxford (1966).

30. W.C. Moshier and G.D. Davis, submitted to Corrosion.

31. R.E. Watsun and M.L. Perlman, Struct. Bonding, 24, 83 (1975).

32. W.F. Egelhoff, Surf. Sci. Rept., 6, 253 (1986).

33. J.A. Davies, J.P.S. Pringle, R.L. Graham, and F. Brown, J. Electrochem. Soc., 109, 999 (1962).

34. A.G. Revesz and J. Kruger, in "Passivity in Metals," R.P. Frankenthal and J. Kruger, Editors, p. 137, The Electrochemical Society, Princeton, NJ (1978).

FIGURE CAPTIONS

Figure 1. Potentiodynamic polarization curves for pure Al and six different sputter-deposited Al alloys.

Figure 2. Variation of the Al 2p and Mo 3d spectra as a function of applied potential for sample AM-2 (Al-7.8Mo): a) As-sputter-deposited, b) at E_{oc} [-931 mV(SCE)], c) at -600 mV(SCE), d) at -400 mV(SCE), and e) at E_b [-4 mV(SCE)].

Figure 3. Variation of the Al 2p and Cr $2p_{3/2}$ spectra as a function of applied potential for sample AC-1 (Al-6.8Cr): a) As-sputter-deposited, b) at E_{oc} [-1125 mV(SCE)], c) at -600 mV(SCE), d) at -400 mV(SCE), and e) at E_b [-232 mV(SCE)].

Figure 4. The Mo^{ox}-to-Al^{ox} ratio as a function of anodic overpotential.

Figure 5. The Cr^{ox}-to-Al^{ox} ratio as a function of anodic overpotential.

END

FEB.

1988

DTIC